JOURNAL
OF THE AMERICAN CHEMICAL SOCIETY

VOLUME 93, NUMBER 7 APRIL 7, 1971

Physical and Inorganic Chemistry

Reversible Reactions of Gaseous Ions. I. Methane–Water System

D. P. Beggs[1a] and F. H. Field*[1b]

Contribution from the Corporate Research Laboratories,
Esso Research and Engineering Company, Linden, New Jersey 07036.

Received July 8, 1970

Abstract: The hydrated proton equilibria, $H(H_2O)_n^+ + H_2O \rightleftharpoons H(H_2O)_{n+1}^+$, were studied in the methane–water system. An extensive effort was made to determine the effects of the instrumental parameters upon the ion intensities and equilibria in this system. Only the repeller and the ion-accelerating voltage affected the equilibrium constants in any way. It is estimated that these factors taken together introduce at most an error of a factor of 2 into our equilibrium constants. Metastable ions associated with ionic water-cluster dissociations were observed, and their dependence upon total pressure was studied. Only two dissociations (n = 4 and 5) had contributions from spontaneous dissociation processes. Cross sections for most of the observed dissociations are tabulated. Thermodynamic values were calculated from the various equilibrium constants and their temperature coefficients. These values compare quite well with previous results from this laboratory and compare well with the work of Kebarle, *et al.*, when n = 3, 4, and 5. Our values for the first two equilibria differ very much from those reported by Kebarle.

In recent high-pressure mass spectrometric studies on benzyl acetate, *tert*-amyl acetate, and water,[2a] substituted benzyl acetates,[2b] and benzene,[3] the spectra contained ions the intensities of which exhibited an inverse dependence upon temperature. The m/e values of these ions were invariably such as to indicate that the ions were formed by association reactions, and from the evidence available we concluded that the reactions occurring were reversible reactions which, indeed, had achieved equilibrium. For example, with benzyl acetate we observed the reaction which is shown in eq 1, which constitutes an $(M + 1)^+$–$(2M + 1)^+$ association reaction. Thermodynamic quantities were calculated from the equilibrium constants for these reactions and from their temperature coefficients.

A disconcerting result was obtained with the acetate esters; namely, the entropies for the association reactions were found to be positive in the range 0–15 cal/(deg mol). Because of the loss of three translational degrees of freedom, association reactions generally exhibit entropy changes on the order of −30 to −50 cal/(deg mol). We were able to find no source of error in these experiments which might have produced these unexpected results. We believe that reversible gaseous ionic reactions are of much interest and potential importance, and, more specifically, our positive entropy findings are unusual and demand further efforts at verification. Therefore, we have undertaken a relatively extensive investigation of reversible gas-phase

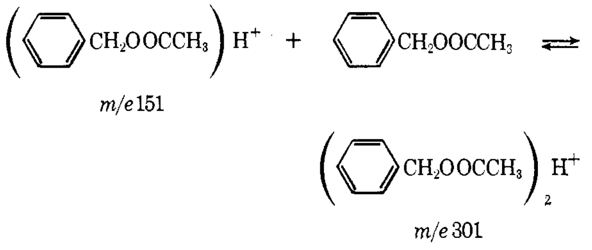

(1)

---

[1] (a) Esso Postdoctoral Fellow; (b) address correspondence to this author at The Rockefeller University, New York, N. Y. 10021.

[2] (a) F. H. Field, *J. Amer. Chem. Soc.*, **91**, 2827 (1969); (b) *ibid.*, **91**, 6334 (1969).

[3] F. H. Field, P. Hamlet, and W. F. Libby, *ibid.*, **91**, 2839 (1969).

ionic reactions in general and our mass spectrometric technique in particular.

Rather than at the present expending further effort on acetate esters, which have been investigated only in this laboratory, we have investigated the reversible reactions in water, for with it comparisons can be made with the published results of Kebarle, Searles, Zolla, Scarborough, and Arshadi[4] (hereafter referred to as Kebarle). Because of our continuing interest in chemical ionization,[5] our experiments have been done under chemical ionization conditions; namely, about 1 Torr of reactant gas and appreciably smaller amounts of the material under investigation (water, in this case). We have also investigated the effects of various instrumental parameters on the reversible reactions, and we have made a mathematical analysis of certain aspects of the reactions occurring in the ionization chamber of the mass spectrometer. The results of these activities will be described in this and subsequent publications. In this paper we concern ourseleves primarily with the methane–water system.

In addition to the work cited above, Kebarle and his coworkers have issued a long series of reports[6–11] on the equilibria occurring in a variety of systems using several different types of apparatus. Water ion clustering reactions and collision-induced water ion declustering reactions have been investigated by DePaz, Leventhal, and Friedman.[12] They report cluster distributions appreciably different from those of Kebarle. They also raise questions about the extent to which equilibrium is achieved in their experiments and, by extension, in other experiments involving reversible gaseous ionic reactions. Ferguson and Fehsenfeld[13,14] and Narcisi and Bailey[15] have considered the reactions producing water ion clusters in the upper atmosphere, but the reactions occurring are generally represented as three-body kinetic processes rather than equilibrium processes.

It has been established[4] that when the hydronium ion (H_3O^+) is formed in a water vapor environment it initiates a reversible reaction sequence which may be represented by the equations

$$H(H_2O)_n^+ + H_2O \rightleftarrows H(H_2O)_{n+1} \qquad (2)$$

The extent to which the several equilibria proceed depends upon pressure and temperature, and in the work reported to date, clusters with n up to 8 have been observed. The constants for the equilibria are given by the expressions

$$K_P = (I_{H(H_2O)_{n+1}^+}/I_{H(H_2O)_n^+})(1/P_{H_2O}) \qquad (3)$$

In the studies to date the H_3O^+ has been produced by the reaction

$$H_2O^+ + H_2O \longrightarrow H_3O^+ + OH \qquad (4)$$

with the H_2O^+ formed either by electron impact, proton impact, or α-particle impact. In the present work H_3O^+ is formed by proton transfer from appropriate reactant ions.

$$RH^+ + H_2O \longrightarrow H_3O^+ + R \qquad (5)$$

Experimental Section

The basic apparatus used for these studies was the Esso chemical physics mass spectrometer described previously.[2a,16] Three different sources have been used: the original source used in this equipment for many years (source I), a slightly modified version of this source (source II), and a new source which can be both cooled and heated (source III). With it the source temperature can be maintained constant at any value from − 195 to +270°.

The electrode arrangement in the new source is depicted in Figure 1. The electrodes are made of 316 stainless steel, and they are positioned and spaced by synthetic sapphire spheres. The filament holder is made of boron nitride. The dimensions of both the electron entrance slit and the ion exit slit are 3.0 × 0.05 mm, and the construction of the ionization chamber is such as to reduce extraneous gas leaks to a minimum. When the pressure of CH_4 in the source is 1.0 Torr, the pressure in the region outside the source is 5–10 × 10^{-4} Torr, depending upon the source temperature, and the corresponding pressure in the analyzer is 2–5 × 10^{-6} Torr.

The distance between the ion exit slit (a) and the focus electrodes (b) is 5.1 mm, and this large distance reduces field penetration into the ionization chamber. The distance between the focus plate and screen (c) is 7.4 mm. The large distance from c to a and the presence of the screen virtually assures little or no potential penetration by the ion-accelerating voltage into the source region and the upper reaches of the ion gun.

The electron collector (6) and electrode (3) were always maintained at the ionization chamber potential. The repeller and focus plates were kept at minimum operating potentials (usually <2.0 V repeller and 5 V focus) for most of the experiments. Thus, these minimal relative potentials in and around the source region produced approximate field-free conditions in the source and for a distance 12 mm downstream in the ion gun.

The ion source can be heated or cooled. The source block was fashioned from a large piece of stainless steel which has a channel running through it. Cooling of the source is accomplished by means of the channel, for it is connected to the exterior of the mass spectrometer vacuum envelope by means of appropriate glass and metal tubing. Nitrogen gas or liquid nitrogen is used as the refrigerant, and the temperature of the block (and thus of the ionization chamber) is controlled by adjusting the temperature and/or flow rate of the nitrogen through the channel. The block is heated by a resistance heater of sufficient capacity to achieve an upper temperature limit of 270°. With either heating or cooling, it is not difficult manually to maintain the temperature at any value with a constancy of ±2°. The temperature is measured by means of a chromel–alumel thermocouple attached to the block and to the cover plate of the ionization chamber. The standard voltage–temperature calibrations were used.

The question of the extent to which the reactant gas achieves temperature equilibrium with the walls of the cavity containing it is of prime importance. We have considered this problem in an earlier work concerned with temperature effects on chemical ionization mass spectrometry,[2a] and we concluded that equilibrium is achieved. We have obtained new data which strengthen this conclusion. It is very convenient to use a Matheson Model 49 subatmospheric pressure regulator to control the pressure of the gas on the high-pressure side of the mass spectrometer gold foil molecular leak. In turn this control results in a control of the pressure in the ionization chamber of the mass spectrometer, and once a settting is made and conditions are maintained constant, the ionization chamber pressure does not vary significantly (less than a few per cent) over long periods of time (on the order of several hours). However, when the temperature of the ionization chamber is changed the pressure in the ionization chamber changes in direct proportion to the temperature change. The pressure is measured by a Texas Instruments, Inc. quartz spiral Bourdon gauge connected

---

[4] P. Kebarle, S. K. Searles, A. Zolla, J. Scarborough, and M. Arshadi, *J. Amer. Chem. Soc.*, **89**, 6393 (1967).

[5] F. H. Field, *Accounts Chem. Res.*, **1**, 42 (1968).

[6] A. M. Hogg, R. M. Haynes, and P. Kebarle, *J. Amer. Chem. Soc.*, **88**, 28 (1966).

[7] A. Good, D. A. Durden, and P. Kebarle, *J. Chem. Phys.*, **52**, 212 (1970).

[8] A. Good, D. A. Durden, and P. Kebarle, *ibid.*, **52**, 222 (1970).

[9] I. Dzidic and P. Kebarle, *J. Phys. Chem.*, **74**, 1466 (1970).

[10] M. Arshadi, R. Yamdagi, and P. Kebarle, *ibid.*, **74**, 1475 (1970).

[11] M. Arshadi and P. Kebarle, *ibid.*, **74**, 1483 (1970).

[12] M. DePaz, J. J. Leventhal, and L. Friedman, *J. Chem. Phys.*, **51**, 3748 (1969).

[13] F. C. Fehsenfeld and E. E. Ferguson, *J. Geophys. Res.*, **74**, 2217 (1969).

[14] E. E. Ferguson and F. C. Fehsenfeld, *ibid.*, **74**, 5743 (1969).

[15] R. S. Narcisi and A. D. Bailey, *ibid.*, **70**, 3787 (1965).

[16] F. H. Field, *J. Amer. Chem. Soc.*, **83**, 1523 (1961).

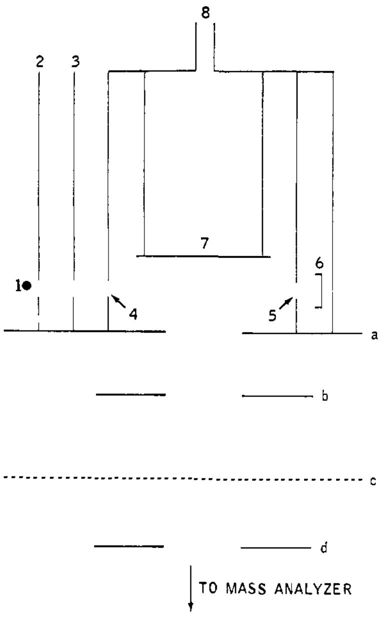

Figure 1. Line diagram of new ion source (source III): (1) filament, (2) and (3) electron gun electrodes, (4) electron entrance slit, (5) electron exit slit, (6) electron collector, (7) ion repeller, (8) gas inlet, (a) ion exit electrode, (b) ion focus electrode, (c) 200-l./in. screen at focus electrode potential, (d) analyzer entrance slit (ground potential).

to the gas inlet line at a point about 1 cm above the ionization chamber. At this point the gas inlet line and the tube leading to the pressure gauge are fabricated from the same piece of metal as the cover of the ionization chamber, and it may fairly be assumed that the temperature of this tube and cover is equal to that measured by the chromel–alumel thermocouple.

We give in Figure 2 a plot of the ionization chamber pressure against the absolute temperature determined by the chromel–alumel thermocouple. These data were taken over a time of about 3 hr, and during this time the pressure controller maintained a constant flow through the system. The linearity of the plot is significant. The observed change in pressure can be the result of a change in the temperature of the gas, a change in the particle density of the gas, or some combination of the two. Changes in particle density in the ionization chamber could result from differential effects of the temperature change on the flow into and out of the ionization chamber, but it seems unlikely that a combined change in the gas temperature and the particle density would give rise to the observed linearity of the pressure–temperature relationship. Furthermore, it might well be that changes in temperature affect the flow into and out of the ionization chamber in about the same way so as to make differential flow effects small. Taking everything into account, we attribute the observed changes in pressure to changes in the temperature of the gas in the ionization chamber, and we consider the linearity shown in Figure 2 to constitute evidence that the gas in the ionization chamber is in temperature equilibrium with the walls of the chamber.

Some experiments on the effects of operating parameters on reversible reactions were made on the original source of the Esso chemical physics mass spectrometer (source I), and others were made on the slightly modified version of this source (source II). The electrode configuration of the original source is very similar to that depicted in Figure 1, except that the screen (item c, Figure 1) is not present. In the modification of the original source to produce source II an extra electrode is inserted between the ionization chamber and the focus electrodes, and this serves to reduce or eliminate penetration of the ion-accelerating potential into the ionization chamber, since this intermediate electrode is operated at the potential of the ionization chamber. Of the three ion sources used, the new source (source III, Figure 1) is the most suitable for the equilibrium studies we have made, but no significant differences in behavior or results have been observed between any of the sources. In our experience, the results do not exhibit a highly sensitive dependence upon the identity of the ionization source.

The electron current emitted from the filament in the quantitative water experiments was in the range 10–50 μA. The electron current was varied so as to maintain the monitored ion current constant at some preselected value, usually 5.0×10^{-13} A. The monitored ion current comprises a fraction of the total ion current (about 10%) collected by a wire inserted into the ion beam between the ion gun and the mass analyzer. The current in the ionization chamber is not known accurately, but it is probably 100–1000 times smaller than the emitted current. The electron-accelerating voltage was 220 V.

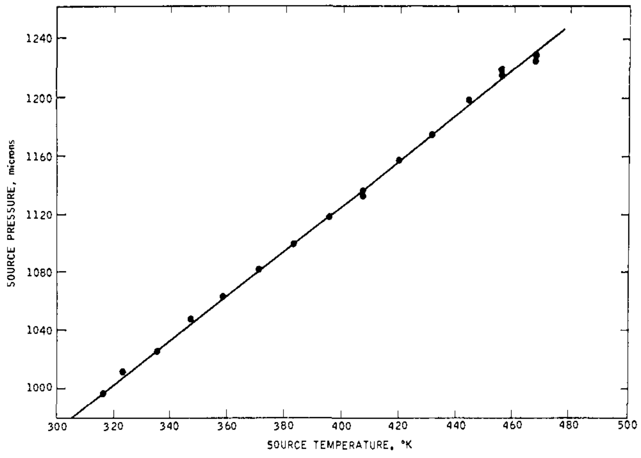

Figure 2. Source pressure *vs.* source temperature; methane gas, source III.

The materials used in this research were laboratory distilled water and Matheson Ultra High Purity methane (99.97%). The mass spectrometer showed that the methane contained trace amounts of water, and these were removed by passing the methane through a bath of refrigerant maintained at an appropriate temperature (−70°).

Results and Discussion

A. Variation of Experimental Parameters. Since a major objective of this research is to determine whether experimental and/or instrumental errors and artifacts can account for the unexpected results obtained previously and referred to above, we will in this section give the results of our investigation of the effect of instrumental parameters on reversible reactions in our mass spectrometer. The results are largely negative in the sense that no unusual or unexpected effects were observed.

The following parameters were varied over appropriate ranges without manifesting an observable effect on appropriately chosen test reversible reactions and/or equilibria: (1) bias voltage on the electron collector electrode, (2) voltage applied to electron collimating magnet, (3) the potential applied to electrode 3 of Figure 1, and (4) the magnitude of the ionizing electron current.

Two types of investigations of the effect of variations in repeller voltage were made. We show in Figure 3 the variation of the monitored ion current with repeller voltage. These data were taken with the new source operating under approximate field-free conditions. In particular the ion focus electrodes were maintained 5 V negative with respect to the ionization chamber. The aspect of the ion-current behavior depicted in Figure 3 which is noteworthy is that it was necessary to apply about 1 V to the repeller to effect the emergence of any ions from the ionization chamber. This type of behavior has been observed in a very large majority of the experiments made, but once in a while very small intensities of ions can be obtained at repeller voltages down to about 0.2 V. In addition the minimum repeller for

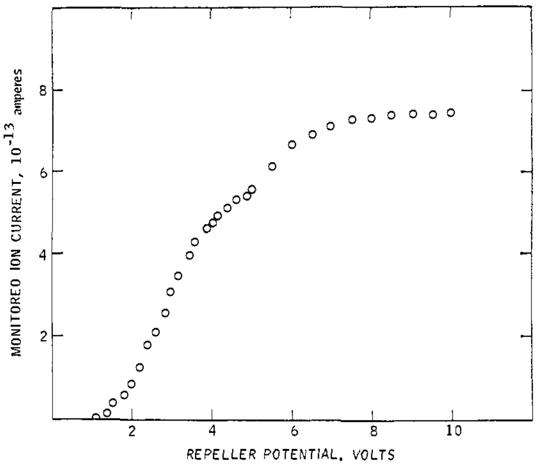

Figure 3. Effect of repeller potential on monitored ion current; source III, propane gas, P_s = 0.970 Torr, source temperature = 42°, emitted electron current = 20 μA.

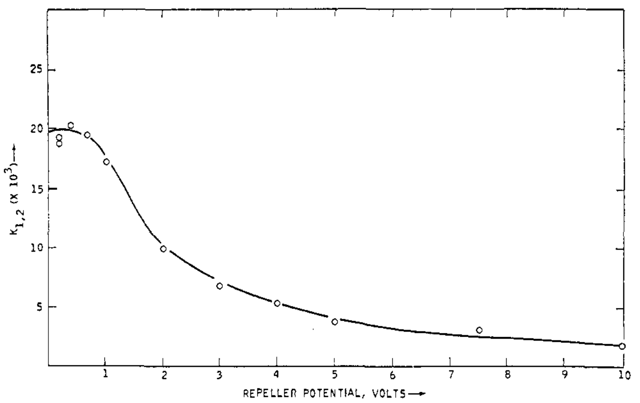

Figure 4. Effect of repeller potential on water equilibrium ($K_{1,2}$); new source, P_{H_2O} = 0.015 Torr, CH_4 reactant, P_{CH_4} = 1.00 Torr, source temperature = 105°, standard state for equilibrium constant = 1 atm.

ion appearance varies in a consistent way with the temperature of the ionization chamber, rising to about 8 V when the ionization chamber is operated at liquid nitrogen temperature.

The other type of repeller voltage experiment is depicted in Figure 4, which shows the effect of repeller voltage on the constant for water equilibrium, namely

$$H_3O^+ + H_2O \rightleftarrows H_5O_2^+ \tag{6}$$

and

$$K_{1,2} = (I_{H_5O_2^+}/I_{H_3O^+})(1/P_{H_2O}) \tag{7}$$

The value of the equilibrium constant decreases by a factor of 10 over the range of repeller voltage investigated (10 V), and a qualitatively similar decrease has been observed previously for benzyl acetate.[2a] However, one observes from Figure 4 that below a repeller voltage of about 1 V no significant change in the equilibrium constant occurs. At the time that the experiment shown in Figure 4 was done, small ion intensities could be obtained at repeller voltages below 1 V, and the data given in Figure 4 in this range were obtained by increasing the sensitivity of the equipment.

The decrease in $K_{1,2}$ above 1 V in Figure 4 may be attributed to the effect on the equilibrium constant of the nonthermal energy derived from the repeller field (collision-induced dissociations), or it may result from the decrease in the ion residence time consequent on the increase in the repeller voltage. Both Figure 3 and Figure 4 indicate that below 1 V the effect of the repeller upon the ionic behavior decreases markedly. The behavior is compatible with a postulate that the ions are held in the ionization chamber by a restraining force, perhaps the negative space charge of the ionizing electron beam or perhaps negative surface charges. In the quantitative experiments made on water the repeller was maintained at a potential of 2.0 V, which is a compromise between the zero voltage desirable for thermodynamic reasons and the finite repeller needed with our machine to obtain a usable sensitivity. We conclude from Figure 4 that equilibrium constants obtained in this way will be lower than the zero-field values by about a factor of 2.

The effect of the focus electrode voltage was investigated in the range 0 to −50 V with respect to the ionization chamber. The voltages referred to are the averages of the slightly different voltages applied to the two halves of the focus electrodes. The experiments were made with source III and approximate field-free conditions. The values of $K_{2,3}$ and $K_{3,4}$ in the water–methane system decreased with increasing voltage by about 25% over the voltage range studied. In the quantitative experiments made on water the focus electrode was maintained 5.0 V negative with respect to the ionization chamber. Values of the equilibrium constants indistinguishable from those at lower potentials were obtained, but the sensitivity of the apparatus was at a usably high value.

A matter of much concern in attempting to make quantitative measurements on reversible gaseous ionic reactions is the possibility that collision-induced decompositions of association ions will occur, which will result in ion intensities which deviate from those corresponding to thermodynamic equilibrium. Such collision-induced decompositions may occur in the ionization chamber, and this possibility has been mentioned in the preceding paragraphs. They may occur in the mass spectrometer analyzer tube, in which case metastable ions will be observed. These have been observed and will be discussed later. Finally, they may occur in the ion gun, and most of the fragment ions thus formed will be effectively lost. However, collisions occurring very near to the ion exit slit of the ion source may produce fragment ions which will appear as a satellite on the low-mass side of the true fragment ion of the same *m/e* value formed in the ionization chamber. Such a satellite peak conceivably could be confused with the true fragment peak. Satellite ions of this kind were observed with our original source (source I) in our study of benzyl acetate,[2a] and in some check experiments on water, disagreements for the values obtained for $K_{1,2}$ and $K_{2,3}$ with those reported by Kebarle[4] were attributed to the occurrence of collision-induced dissociations. In our new source the purpose of the fine mesh screen (item c, Figure 1) and the small potential difference between source and focus electrode is to eliminate collision-induced dissociations in the ion gun. With this source no satellite peaks have been observed; all peaks occurring at integral *m/e* values have the proper shape, and in general no evidence or even suspicion exists that the intensities used in equilibrium

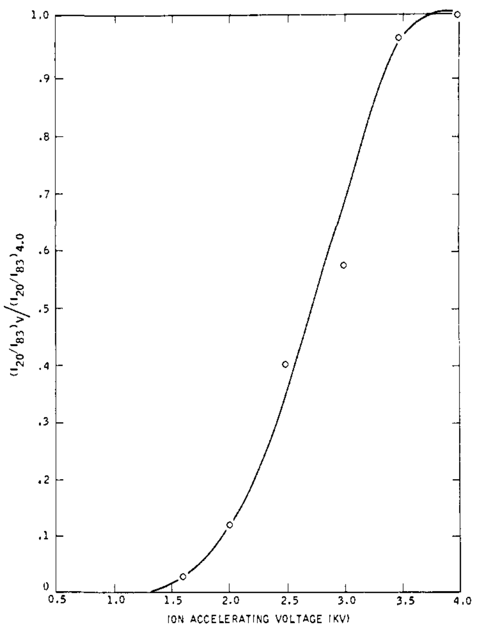

Figure 5. Mass discrimination effect; Ne–Kr mixture.

constant calculations contain a collision-induced component. We shall see that the values obtained in this work for $K_{1,2}$ and $K_{2,3}$ of the water system are also in disagreement with those of Kebarle,[4] and thus special attention has been paid to the forms of the peaks at *m/e* 19, 37, and 55. No untoward behavior is observed.

The effect of ion-accelerating voltage on the collection efficiency of ions of rather widely different mass was investigated using source II. A mixture of neon and krypton was introduced into the source and ionized by electron impact. The ratio of the intensity of the *m/e* 20 ion to that of *m/e* 83 was determined at several ion accelerating voltages between 1.5 and 4.0 kV. Mass discrimination effects have been known in mass spectrometry for many years, but we are still surprised at the magnitude of the discrimination which we observe. The quantity $(I_{20}/I_{83})_{\text{KV}}/(I_{20}/I_{83})_{4.0}$ is plotted against ion-accelerating voltage in Figure 5. The ordinate is the ratio of the ratios determined at the ion voltage KV and at 4.0 kV. *m/e* 20 and *m/e* 83 were chosen to represent masses which are typical and important in the water system, namely, *m/e* 19, H_3O^+, and *m/e* 73, $H_9O_4^+$. Not much change in the ratio occurs between 3.5 and 4.0 kV, suggesting that little discrimination occurs above 3.5 kV. However, from 3.5 to 2.0 kV the loss of the lower mass ion increases by a factor of 10. In the quantitative measurements made on water the ion-accelerating voltage was maintained at 3.0 kV, and from Figure 5 we conclude that some loss (probably less than a factor of 2) of the lower mass ions occurred.

In summary, of the instrumental parameters we have investigated, the ion-repeller voltage and the ion-accelerating voltage had differential effects on the intensities of different ions, and the magnitudes of these effects were on the order of factors of 2, and in opposite directions. Thus we are of the opinion that equilibrium constants determined with our machine and technique may be in error by about a factor of 2 as a loosely established upper limit.

B. The System Methane–Water. A variety of exploratory experiments were made with the methane–water system using the three kinds of ion sources described above and some variety of experimental conditions, but our major effort was invested in two extensive, replicate investigations of the effect of both pressure and temperature on the spectra of methane–water mixtures. We will present only data obtained in these experiments, and we can summarize the results of the other experiments by saying that in general they corroborate the results of the pressure–temperature studies. The total body of concordant data on the methane–water system is large.

The pressure–temperature studies were made using source III operated under approximate field-free conditions as defined previously. The pressure of methane in the ionization chamber was established at a source temperature of 0° at 1.00 ± 0.03 Torr, and varied with temperature according to Charles' law (Figure 2). Water vapor was mixed with the methane in the inlet line to the ion source, and the total pressure in the source varied with the amount of water added. Spectra were determined at water partial pressures of 0.0007, 0.015, 0.045, 0.075, 0.100, 0.150, and 0.200 Torr and at ion source temperatures of 0, 40, 80, 120, 160, 200, and 240°, a total of 49 determinations being made over a period of several days. A replicate determination was made about a week later, so a grand total of 98 determinations was made. The agreement between the replicate determinations was good, and in general average values will be given in this paper.

We give in Table I spectra of the methane–water system at four ion source temperatures. We call attention to the hydrated proton ions at *m/e* 19, 37, 55, 73, 91, and 109. Initially H_3O^+ is formed by reaction 5, where, in the methane system, RH^+ consists of about equal amounts of CH_5^+ and $C_2H_5^+$, and the higher hydrates are formed by reactions 2. As the temperature decreases the intensities of the higher hydrates increase at the expense of the lower hydrates, but even at 0°, H_3O^+ has a large intensity (0.198). This point is of impor-

Table I. Spectra Obtained in the Methane-Water System[a]

		Relative intensity			
m/e	Ion	0°	80°	160°	250°
17	CH_5^+	0.017	0.032	0.066	0.093
19	H_3O^+	0.198	0.528	0.713	0.609
28	$C_2H_4^+$	0.020	0.031	0.031	0.036
29	$C_2H_5^+$	0.030	0.061	0.118	0.162
35	$(CH_4H_2O)H^+$	0.006			
37	$H(H_2O)_2^+$	0.154	0.169	0.022	0.017
41	$C_3H_5^+$	0.038	0.064	0.040	0.074
43	$C_3H_7^+$	0.014	0.017	0.008	0.009
55	$H(H_2O)_3^+$	0.120	0.080	0.002	
73	$H(H_2O)_4^+$	0.279	0.015		
75		0.002			
77		0.004	0.002		
82		0.004	0.001		
91	$H(H_2O)_5^+$	0.090			
95		0.006			
97		0.004			
100		0.004			
109	$H(H_2O)_6^+$	0.003			
113		0.005			

[a] P_{CH_4} = 1.00 Torr, P_{H_2O} = 0.015 Torr, approximate field-free conditions.

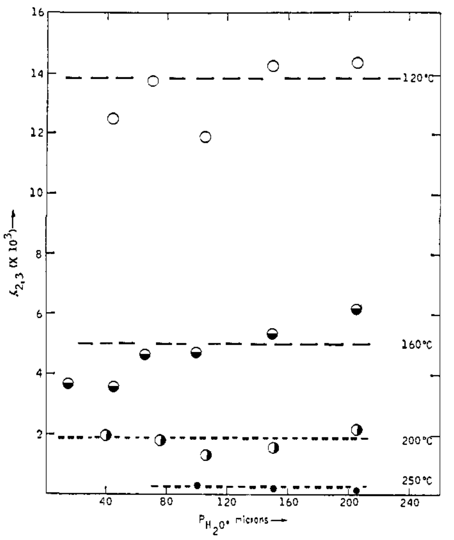

Figure 6. Equilibrium constants for $H_5O_2^+ + H_2O \rightleftarrows H_7O_3^+$; 120, 160, 200, 250°.

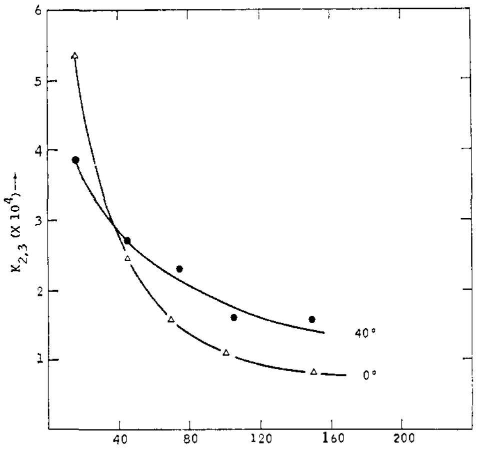

Figure 7. Equilibrium constants for $H_5O_2^+ + H_2O \rightleftarrows H_7O_3^+$; 0, 40°.

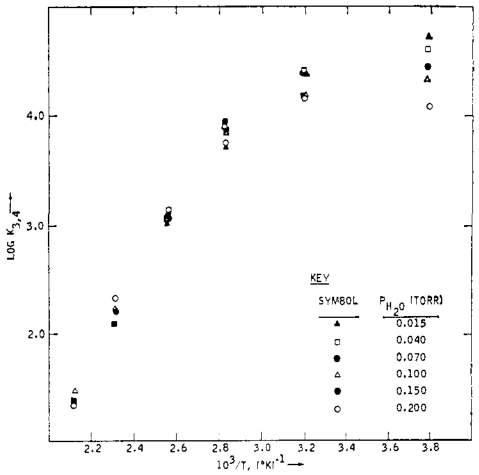

Figure 8. van't Hoff plot for $H_7O_3^+ + H_2O \rightleftarrows H_9O_4^+$.

tance and will be returned to later. Tabulations similar to Table I but at higher water partial pressures show higher intensities for the higher hydrates.

If equilibria are established between the several hydrates, the appropriate equilibrium constants calculated from eq 3 should be independent of water pressure. We find unexpected behavior. For some ions and under some conditions a constancy of equilibrium constants indicative of the attainment of equilibrium is observed. We give an example of this kind of behavior in Figure 6, which comprises plots of $K_{2,3}$ as a function of water pressure at different temperatures. Fluctuations which we ascribe to experimental error are to be observed, but no significant trends occur. For other ions and other conditions significant trends in the equilibrium constants occur, and typical examples of this type of behavior are given in Figure 7. The unexpected aspect of this behavior is the decrease in the equilibrium constants as the water pressure is increased. One could easily understand the occurrence of a reverse trend, that is, an increase in the equilibrium constant with increasing pressure, for this would reflect the approach to equilibrium of an initially kinetically limited system. However, we have never observed a trend of this kind in any of our studies involving chemical ionization conditions.

The occurence of the inconstant behavior depicted in Figure 7 is reproducible, and we have observed it in other systems, in particular propane–water, neat water, and neat methane at low temperature. The phenomenon has some generality, at least in our equipment, and it clearly has a more profound origin than occurrence of a random error. For the methane–water system we observe that constancy of equilibrium constants tends to occur for higher temperatures and/or higher hydrates, and inconstancy tends to occur at the converse conditions. As the temperature is increased the inconstancy in the *K* value for a given equilibrium decreases and disappears, or, alternatively, comparing the *K* values for a series of equilibria at the same temperature, the degree of inconstancy is greater for the lower hydrates. Thus the $K_{1,2}$ values are constant only at temperatures of 200° and higher, whereas the $K_{5,6}$ values are constant even at 0°. Generalizing, the quantity which seems to be most important in this matter is the degree of reaction. If the temperature and/or identity of the equilibrium are such that an equilibrium lies far on the side of the products, inconstant behavior is observed. The degree of inconstancy observed is less if the equilibrium concentrations of product and reactant are about of equal size, and good constancy is observed when the equilibrium concentration of product is 10% or less that of the reactant.

We conclude that equilibrium is not established under circumstances when inconstant behavior of the equilibrium constants is observed, and we believe that the failure to achieve equilibrium is the result of the fact that the ions have a limited residence time in the ionization chamber. The problem of limited residence time is exacerbated when the system is such that multiple, sequential equilibria must be established. On the other hand, we believe that equilibrium is established under circumstances when the equilibrium constants are indeed constant. We shall deal more quantitatively with the problem of the establishment of equilibrium under chemical ionization conditions in a later paper.

A second way of representing the data in the methane–water system pressure–temperature study is to construct van't Hoff plots of the equilibrium constants

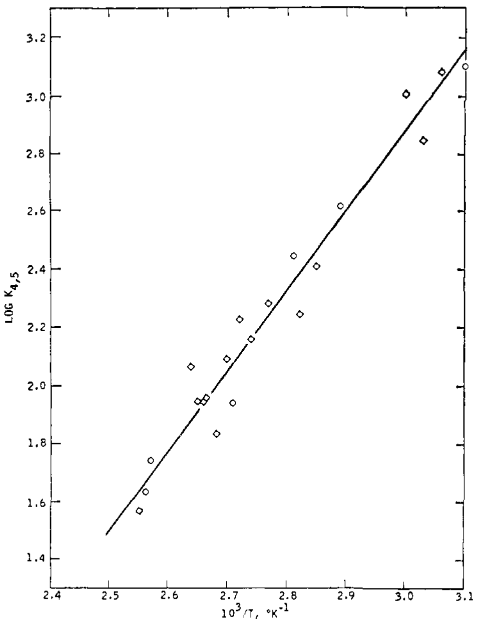

Figure 9. van't Hoff plot for $H_9O_4^+ + H_2O \rightleftarrows H_{11}O_5^+$.

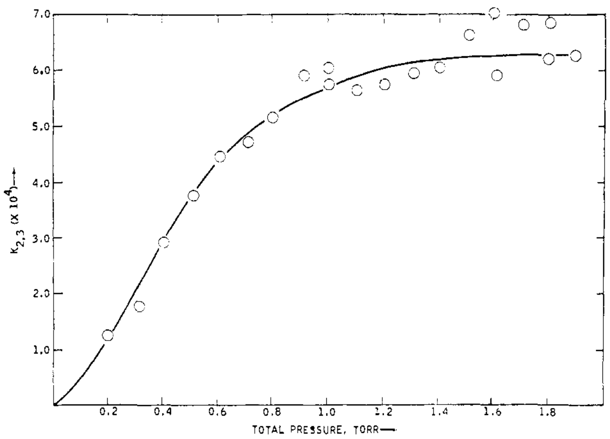

Figure 10. $K_{2,3}$ *vs.* total pressure; $P_{H_2O} = 0.015$ Torr, P_{CH_4} = variable, source temperature = 0°.

for the various reactions, including in the plots equilibrium constants obtained at several different water pressures. We give in Figure 8 an example of such a plot. The plots generally have the form of a cornucopia, for at low temperatures the values of the equilibrium constants obtained depend upon the water pressure, and the plot flares out. The extent of the flaring depends upon the equilibrium being considered, and it is worse for the lower equilibria. In general the van't Hoff plot for a particular reaction at a particular water pressure exhibits a linear portion at high temperatures and a curved portion (concave downward) at low temperatures. It is clear that the same nonequilibrium phenomenon which causes the inconstant behavior of the equilibrium constants with pressure causes the flaring and curving of the van't Hoff plots. On the other hand, we believe that equilibrium is established under conditions where the equilibrium constants are independent of pressure and the van't Hoff plots are linear. If this be the case, the linear portions of the van't Hoff plots can be used to calculate thermodynamic quantities for the corresponding equilibria. A typical linear plot for a higher equilibrium is given in Figure 9. By going to sufficiently low pressure (0.0007 Torr) it is possible to obtain linear van't Hoff plots even for $K_{1,2}$ values.

It is desirable to investigate the effect of methane pressure on the equilibrium constants for reaction 2. A typical result is given in Figure 10, which shows the variation of $K_{2,3}$ with methane pressure with a fixed amount of water. Similar curves were obtained for the 1,2; 3,4; and 4,5 equilibria. No significant variations in the K values occur above a total pressure of approximately 1 Torr. From an operational point of view this means that above 1 Torr the total pressure is not a significant variable which must be carefully controlled; that is, the effect of total pressure on the equilibrium constants has become constant. The decreases in K values at lower pressures may be the results of corresponding decreases in the ion residence times in the ionization chamber. The ion drift velocity is inversely proportional to the pressure at constant electric field strength, which is the case in these experiments. Then as the pressure decreases the time available for the occurrence of the forward reactions in (2) decreases, and smaller amounts of products are formed. Equilibria are not attained. The corollary of this is that above 1 Torr residence time no longer affects the amount of reaction occurring, which is compatible with the postulate that above 1 Torr equilibria are established in reactions 2.

We give in Table II thermodynamic values for the various hydrated proton equilibria calculated from the linear portions of the several van't Hoff plots. For comparison we include in Table II thermodynamic values found by Kebarle and coworkers[4] and in an earlier study in this laboratory.[2a] The Kebarle experiments were made either with neat water or in water with argon added at total pressures up to about 5 Torr. The earlier experiments in this laboratory were made with neat water at a pressure of 0.50 Torr using the original ion source (source I). The most directly measured and therefore the most meaningful quantities are the equilibrium constants and the free energy changes. The difficulties involved in these experiments are such that we consider agreement of equilibrium constants to within a factor of 2 to be good. Discrepancies of an order of magnitude or more are looked upon as significant disagreements.

With this criterion, very satisfactory agreement exists among all three sets of data for $K_{3,4}$, $K_{4,5}$, $K_{5,6}$, and the corresponding ΔG values. Acceptable agreement exists between the two results for $K_{2,3}$ obtained in this laboratory; the Kebarle value is significantly higher. The discrepancy between the Kebarle value for $K_{1,2}$ and ours is enormous—approximately 13 orders of magnitude. The agreement between the three sets of values for ΔH and ΔS is acceptable for the 3,4 and 4,5 equilibria. The entropy difference obtained in the present work for the 5,6 equilibrium is much less negative than Kebarle's, but the enthalpy change is also less negative. Because of the compensation the agreement of the free energy changes and the equilibrium constants is acceptable. A similar discrepancy is found for the 2,3 equilibrium, but this time the disagreement is between the present results and both Kebarle's results and the earlier results from this laboratory. We do not understand the reason for these discrepancies, but the experimental determinations of enthalpies and entropies

Table II. Experimental Thermodynamic Values for Hydrated Proton Equilibria

$$H(H_2O)_n^+ + H_2O \rightleftharpoons H(H_2O)_{n+1}^+$$

	$-\Delta G_{300}$, kcal/mol			K_{300}[a]			$-\Delta H$, kcal/mol			$-\Delta S$, eu		
$n, n+1$	K[b]	F[c]	B + F[d]	K	F	B − F	K	F	B + F	K	F	B + F
1, 2	25		7.7	1.8×10^{18}		4.2×10^5	36		7	33.3		−1
2, 3	13.6	10	9.3	8.7×10^9	2.3×10^7	6.3×10^6	22.3	20	13	29	31	14
3, 4	8.5	8.2	8.4	1.6×10^6	8.6×10^5	1.4×10^6	17	16.2	16.8	28.3	26.7	28
4, 5	5.5	5.2	4.8	1.0×10^4	8.8×10^3	3.2×10^3	15.3	14.8	12.9	32.6	31.7	28
5, 6	3.9		3.4	710		306	13		8.5	30.3		17

[a] Standard state = 1 atm. [b] Kebarle and coworkers, ref 5. [c] Field, reference 2a. [d] This work.

separately are relatively difficult and the discrepancies may simply reflect experimental error.

We wish to defer part of the discussion of our results until after the presentation of our results for the propane–water system, which is given in a later paper. For the present we remark that we cannot draw unambiguous general conclusions about the validity of our results (and perhaps also about the validity of Kebarle's). We compare our results with those of Kebarle because from the description given of his work,[4] the apparatus used seems suitable for the experiments made, the experiments appear to be well executed, and the results obtained appear to be reasonable. The agreement obtained for the 3,4, 4,5, and 5,6 equilibria indicate that under certain circumstances, at least, our apparatus and technique are as capable as Kebarle's for obtaining thermodynamic data from gaseous ionic equilibria. We point out without further comment at this time that DePaz, Leventhal, and Friedman[12] have expressed doubts that true thermodynamic equilibrium is or can be attained in experiments such as Kebarle's. This criticism, if valid, is also applicable to our experiments.

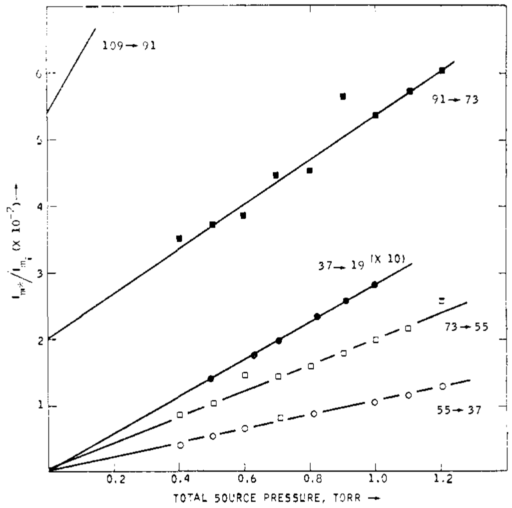

Figure 11. Dependence of metastable ion intensities upon total source pressure; P_{H_2O} = 0.015 and 0.200 Torr, source temperature = 40°.

This agreement for the higher equilibria makes it difficult to understand the disagreement for the 1,2 and 2,3 equilibria. In our earlier work[2a] we attributed the discrepancy in the 2,3 equilibrium between Kebarle's results and ours to the occurrence of collision-induced stripping reactions in our experiments. Since in the present work we obtain the same results with an apparatus in which the likelihood of such stripping is much reduced, we no longer think that this explanation is valid. The discrepancy between our $K_{1,2}$ value and that of Kebarle is so large as to defy explanation. A point to remember is that Kebarle's data for this equilibrium were taken at very high temperatures (400–600°) and a relatively high water pressure, whereas ours were taken between 0 and 250° using a correspondingly lower water pressure. Thus the discrepancy is between our results and an extrapolation of Kebarle's data. Another and more qualitative manifestation of the discrepancy are the spectra given in Table I. According to the equilibrium constant at 300°K given by Kebarle, the m/e 19 intensity in the 0° spectrum should be approximately 5×10^{-14} that of the m/e 37 ion, whereas in fact the intensities are of about equal size. DePaz, Leventhal, and Friedman[12] remark that their water spectra are more displaced to the lower hydrates than would be expected from Kebarle's equilibrium constants.

C. Metastable Ions in the Methane–Water System. The investigation of the effect of methane pressure on the magnitudes of the equilibrium constants (Figure 10) provided some information about metastable ions in the methane–water system. The spectra obtained in this system contain peaks at nonintegral mass numbers, which are clearly formed from ions produced in the field-free region of the analyzer tube between the ion gun and the magnetic field. We shall see that these ions are predominantly collision induced, but we shall refer to them by the generic name of metastable ions. We are concerned in this section only with the metastable ions formed from the water hydrates.

Metastable ions are observed corresponding to the loss of all possible numbers of water molecules save one from all hydrates up to and including $H(H_2O)_5^+$; that is, metastable ions corresponding to the loss of one to four water molecules from $H(H_2O)_5^+$ are observed, and so forth. A metastable corresponding to the loss of H_2O from $H(H_2O)_6^+$ is also observed. The intensities of some of these metastables are too small to be treated quantitatively. Information about the metastables which are large enough to be treated quantitatively is given in Table III and Figure 11. The intensities of the metastables are taken as an approximation to be equal to the height of the highest point in the metastable peak, and these intensities vary with the pressure in the ion source. Plots of ratios of the intensities of several metastable ions to the intensities of the initial ions from which they are formed are given in Figure 11. The pressure in the analyzer tube of the mass spectrometer is linearly related to the source pressure, and thus the plots given in Figure 11 are equivalent to plots of

Table III. Metastable Ions[a]

Metastable transition	m^*	$10^3 \times$ I_{m^*}/I_{m_i}	Q,[d] A^2
Loss of H_2O			
$H(H_2O)_6^+ \rightarrow H(H_2O)_5^+ + H_2O$ 109 91	75.9	102[b]	320
$H(H_2O)_5^+ \rightarrow H(H_2O)_4^+ + H_2O$ 91 73	58.6	40[b]	125
$H(H_2O)_4^+ \rightarrow H(H_2O)_3^+ + H_2O$ 73 55	41.4	22[b]	69
$H(H_2O)_3^+ \rightarrow H(H_2O_2)^+ + H_2O$ 55 37	24.9	13[b]	41
$H(H_2O)_2^+ \rightarrow H_3O^+ + H_2O$ 37 19	9.8	3.4[c]	10.6
Loss of $2H_2O$			
$H(H_2O)_5^+ \rightarrow H(H_2O)_3^+ + 2H_2O$ 91 55	33.3	10.2[b]	32
$H(H_2O)_4^+ \rightarrow H(H_2O)_2^+ + 2H_2O$ 73 37	18.8	5.1[b]	16
Loss of $3H_2O$			
$H(H_2O)_5^+ \rightarrow H(H_2O)_2^+ + 3H_2O$ 91 37	15.1	4.1[b]	13
$H(H_2O)_4^+ \rightarrow H_3O^+ + 3H_2O$ 73 19	4.9	1.4[b]	4.4

[a] Source temperature = 40°. [b] Source water pressure = 0.200 Torr. [c] Source water pressure = 0.015 Torr. [d] $Q = (I_{m^*}/I_{m_i})/(1/Nl)$, where N = gas number density and l = length of dissociation region.

intensity ratios against analyzer pressure. The actual pressure in the analyzer was measured only by means of an ion gauge, and the gauge constant of it is not known. However, as an approximation to obtain rough estimates of the cross sections for the collision-induced dissociations, we use the gauge constant provided by the manufacturer, which presumably refers to air. The resultant error in the pressure determination is probably within a factor of 2, and relative values of cross sections are unaffected. The distance in which the metastables are formed is approximately 20 cm (distance between the entrance to the analyzer and the magnetic field), and this value is used in calculating dissociation cross sections. The cross sections calculated from the observed metastable intensities, the analyzer tube pressure, and the 20-cm distance are given in Table III.

One observes from Figure 10 that the transitions 37 → 19, 55 → 27, and 73 → 55 are all completely collision induced, but the finite intercept in the 91 → 73 plot shows that it is partially collision induced and partially spontaneous. We also give in Figure 10 the lowest portion of the plot for the transition 109 → 91, and this transition also has a spontaneous component. All of the transitions for which more than one water molecule is lost are completely collision-induced. It is of interest, and perhaps of significance, that the two cases where spontaneous decompositions occur involve ions having more water molecules than the four needed to fill the first solvation shell around the proton.

The cross sections listed in Table III vary markedly from one reaction to another. For the loss of any given number of water molecules the cross sections decrease as the size of the decomposing ion decreases. For a given ion decomposing the cross section decreases as the number of water molecules lost increases. Although the absolute values of the cross sections are estimated to be uncertain by a factor of 2 because of pressure uncertainties, the cross sections for some of the processes involving loss of one water molecule are remarkably large. DePaz, Leventhal, and Friedman[12] give plots which indicate that the collision-induced loss of more than one water molecule occurs with a smaller cross section than the loss of only one. They also find that the amount of collision energy needed to effect a decomposition decreases as the size of the decomposing ion increases; this is perhaps equivalent to our finding that at constant energy (3.0 kV) the cross section increases with ion size.

We can offer a possible explanation for the trends we observed in the cross sections for the collision-induced dissociations; namely, the cross sections are an inverse measure of the tightness with which the water molecules are bound in the dissociating ions. These cross sections should then correlate with the corresponding enthalpies for the equilibrium reactions as tabulated in Table II, and, indeed, the trends in the enthalpies found by Kebarle and coworkers[5] agree very well with the trends in cross sections for the loss of one water given in Table III. The enthalpy trend found in this investigation does not correlate, and we consider that our cross-section results support Kebarle's enthalpies. We will consider this matter again in connection with our study of the propane–water system reported in the subsequent paper.